Detailed partial load investigation of a thermal energy storage concept for solar thermal power plants with direct steam generation

M. Seitz, S. Hübner, and M. Johnson

Citation: AIP Conference Proceedings **1734**, 050042 (2016); doi: 10.1063/1.4949140
View online: http://dx.doi.org/10.1063/1.4949140
View Table of Contents: http://scitation.aip.org/content/aip/proceeding/aipcp/1734?ver=pdfcov
Published by the AIP Publishing

Detailed Partial Load Investigation of a Thermal Energy Storage Concept for Solar Thermal Power Plants with Direct Steam Generation

M. Seitz[1, a)], S. Hübner[2] and M. Johnson[3]

[1] *M.Eng., Project Engineer, German Aerospace Center (DLR), Institute of Engineering Thermodynamics, Pfaffenwaldring 38-40, 70569 Stuttgart, Germany.*
[2] *Dipl.-Ing., Project Manager, Linde AG, Seitnerstraße 70, 82049 Pullach, Germany.*
[3] *Dipl.-Ing., Project Manager, German Aerospace Center (DLR), Institute of Engineering Thermodynamics, Pfaffenwaldring 38-40, 70569 Stuttgart, Germany.*

[a)] Corresponding author: markus.seitz@dlr.de

Abstract. Direct steam generation enables the implementation of a higher steam temperature for parabolic trough concentrated solar power plants. This leads to much better cycle efficiencies and lower electricity generating costs. For a flexible and more economic operation of such a power plant, it is necessary to develop thermal energy storage systems for the extension of the production time of the power plant. In the case of steam as the heat transfer fluid, it is important to use a storage material that uses latent heat for the storage process. This leads to a minimum of exergy losses during the storage process. In the case of a concentrating solar power plant, superheated steam is needed during the discharging process. This steam cannot be superheated by the latent heat storage system. Therefore, a sensible molten salt storage system is used for this task. In contrast to the state-of-the-art thermal energy storages within the concentrating solar power area of application, a storage system for a direct steam generation plant consists of a latent and a sensible storage part. Thus far, no partial load behaviors of sensible and latent heat storage systems have been analyzed in detail. In this work, an optimized fin structure was developed in order to minimize the costs of the latent heat storage. A complete system simulation of the power plant process, including the solar field, power block and sensible and latent heat energy storage calculates the interaction between the solar field, the power block and the thermal energy storage system.

INTRODUCTION

In a concentrating solar power (CSP) plant with direct steam generation (DSG) as described in [1], no additional heat transfer fluid (HTF) for the heat transfer from the solar field to the power block (PB) is necessary. This allows for higher steam parameters and enables a much better cycle efficiency in the PB. Such a DSG power plant was built in Kanchanaburi, Thailand in 2010/11 and has been operated thus far for several years. In contrast to state-of-the-art CSP trough technology with a synthetic oil as the HTF as in Andasol 3 [2], no commercial thermal energy storage (TES) systemis currently available for DSG power plants. Due to this, the power plant in Kanchanaburi was developed without a TES.

A previous study [3] determined the economic potential of DSG power plants through a parametric study with sixty different power plant configurations at three different sites. The configuration with a live steam temperature of 500 °C and a live steam pressure of 100 bar reveals the lowest levelized costs of electricity (LEC) costs for a 50 MW power plant. Within the so-called DIVA project, no TES was investigated in the case study. Another study [4] on DSG power plants compares the state-of-the-art oil CSP plant with several DSG configurations, including different TES approaches. As a result, it was determined that there is a potential for cost reduction within the PCM storage system. With an optimized TES, there would be a possible LEC reduction up to 9 % compared to the state-

SolarPACES 2015
AIP Conf. Proc. 1734, 050042-1–050042-8; doi: 10.1063/1.4949140
Published by AIP Publishing. 978-0-7354-1386-3/$30.00

of-the-art oil system. Furthermore, it was reported that the storage capacity of a DSG power plant is slightly smaller compared to that of an oil system.

DSG can be performed with different CSP technologies, i.e. parabolic troughs or tower systems. An advantage of tower systems is the possibility for relatively high live steam parameters within the DSG solar receiver. This enables the implementation of a sensible 2-tank storage system. One approach for such a TES system was developed in [5]. Most of the latent energy of the live steam is not used for storage charging, which is a non-negligible disadvantage of this storage system. Based on this, the charging process takes six hours longer than the discharging process.

Due to the lower live steam pressure during the discharging process [5,6,7,8], it is not possible to generate the rated electrical power output of the PB. Based on this situation, the cycle efficiency drops during discharging to approximately 70-90 %, depending on the implemented storage concept. In [9], a 2-tank system with sensible molten salt was used to develop a high pressure (HP) bypass operating mode for the steam turbine, to generate the rated electrical output power during the discharge mode.

The study [8] presents a wide comparison of TES for DSG systems. This includes steam accumulators and several PCM design concepts with different PCM materials. For a CSP application with DSG, a TES providing heat at constant temperatures for evaporation and condensation of steam is required. As a result, a storage module with sodium nitrate ($NaNO_3$) as the phase change material (PCM) was developed and tested in [6,10,11].

For the steam turbine, superheated steam is required. Therefore, the storage system needs to discharge superheated steam. In order to meet this requirement, a sensible 3-tank storage system was designed in [7], using a nearly eutectic mixture of potassium nitrate (KNO_3) and sodium nitrate ($NaNO_3$) as the sensible storage material. Until now, no detailed system simulation of such a TES was calculated. In [12], only a highly simplified PCM model with $NaNO_3$ as the storage material was presented and used for the system optimization.

This paper shows the development of a DSG TES system, consisting of a PCM storage and a sensible 3-tank storage system at full commercial scale using a system simulation model for optimization of the complete coupled power plant system. Therefore, a PB was developed based on the results in [7,13]. This PB was coupled to the TES system during discharging, operating in a sliding pressure mode. For the simulation of the characteristic behavior of the PCM storage part, a detailed transient numerical simulation was performed with an optimized fin geometry. This fin geometry is necessary to overcome the very low thermal conductivity of $NaNO_3$. With this characteristic line, a quasi-stationary model for the PCM storage was developed. For the simulation of the sensible 3-tank storage system for steam superheating purposes during discharging, a quasi-stationary Ebsilon model was used to describe the partial load behavior of the heat exchangers.

DESCRIPTION OF THERMAL ENERGY STORAGE SYSTEM

Based on early conceptual work in [4], four different more detailed TES system approaches were developed within the DSG-Store project at DLR. These approaches were presented in [7] and differ primarily in the number of storage tanks. The basic system analyzed uses a 3-tank sensible storage system for pre- and superheating of water/-steam. The evaporation is done inside a PCM storage module. Due to the adverse specific heat characteristics of superheated steam, a second 3-tank system was developed to reach a higher temperature within the hot molten salt storage tank. This is feasible since the temperature of the third intermediate tank is raised to pair with the molten salt and the water/steam side of the heat exchanger. Both remaining systems are designed with a 2-tank storage system and are very ambitious and innovative concepts. For the further work in this paper, the 3-tank system with the raised tank temperature was investigated as the best TES system option for a medium-term solution. For that reason, the temperature of the live steam was lowered to 535 °C, to enable a realistically timed market launch for DSG storage systems.

As a reference DSG power plant (see Tab. 1), a parabolic trough power plant with an electrical gross power of 50 MW was selected. The live steam temperature is 535 °C and three different pressure levels, depending on the temperature difference inside the PCM storage system during charging, are considered. The storage system is designed for a discharging time of 7 h. The design of the TES was calculated for a solar multiple of 2. This means that the TES is constructed for the same water/steam mass flow as the PB at nominal operating conditions.

To avoid a minimum steam fraction below 85 % at low pressure turbine outlet [13], indirect reheat was introduced between the high pressure and the low pressure turbine stages. Within this steam/steam heat exchanger, live steam from the SF respectively the TES is used to reheat the turbine steam mass flow.

TABLE 1. Design parameters of the DSG reference power plant.

	Value	Unit
Gross electrical power	50	MW
Live steam temperature	535	°C
Temperature difference during charging	10, 15, 20	K
Live steam pressure	109, 116, 124	bar
Storage discharge time	7	h
Solar multiple	2	-
Condenser pressure	80	mbar

During charging, superheated steam from the SF is conducted to the TES system and the PB, which is at its nominal operating point during the whole charging process. The feedwater from the TES system and the PB is recirculated to the SF hereafter. If the TES system is switched to discharging, feedwater from the PB is evaporated and superheated inside the TES system. The produced live steam is fed into the steam turbine respectively the reheater and is used for electricity generation after sunset or during interruptions of solar irradiance.

The storage system (see Fig. 1 (a)) as presented in [7], consists of a latent heat thermal energy storage (LHTES) and a sensible heat thermal energy storage (SHTES) system. The LHTES is drafted as a shell-and-tube heat exchanger, in which the PCM $NaNO_3$ (see material properties in Tab. 2) is in the shell side of the PCM tank. For a better heat transfer through the PCM, different longitudinal aluminum fin structures connected to the heat exchanger pipes are investigated within this work. Inside the heat exchanger pipes, water/steam is used for the charging and discharging process of the TES system.

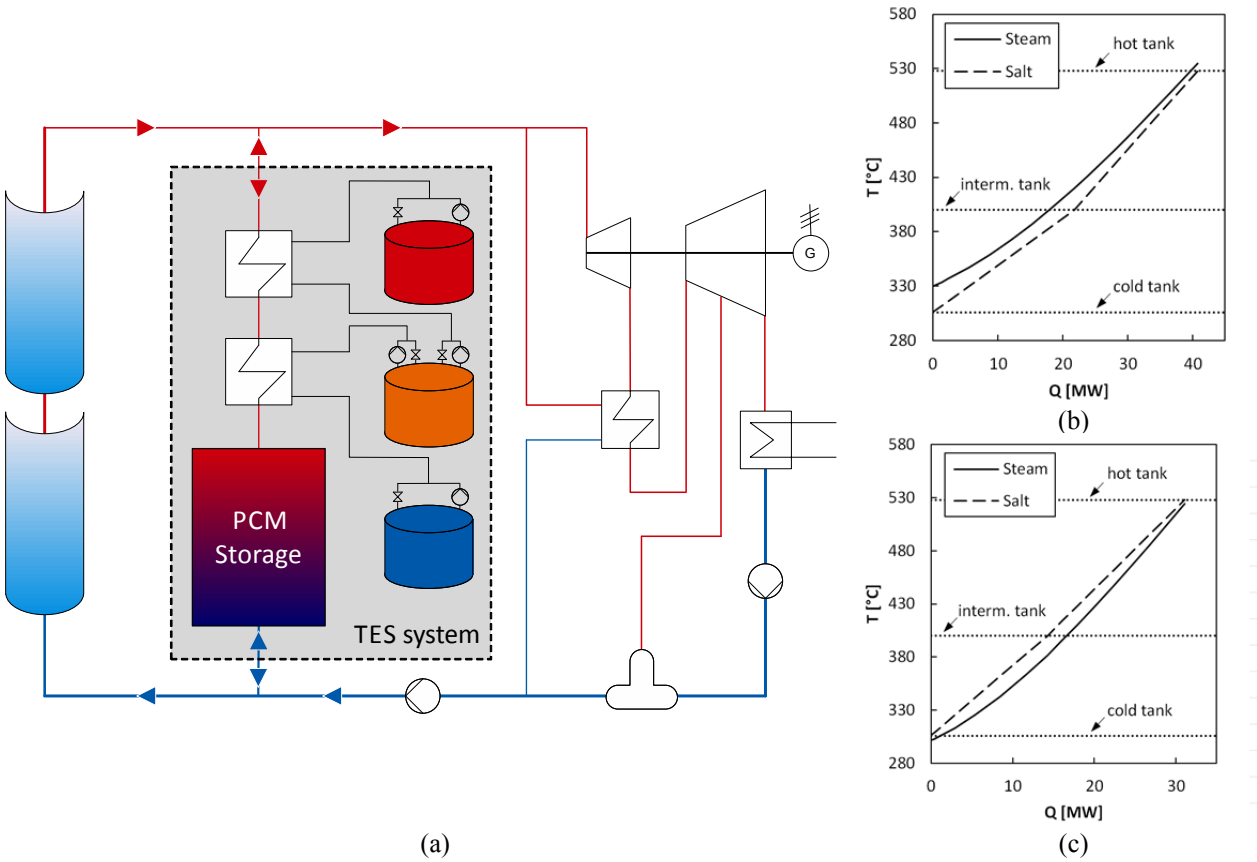

FIGURE 1. (a) Schematic layout of the DSG power plant with thermal energy storage system, consisting of a latent and a sensible heat thermal energy storage system (LHTES and SHTES). (b) Q-T-diagram for the charging and (c) discharging process of the SHTES.

The sensible energy of the water/steam side is stored in a binary mixture of 60 wt-% $NaNO_3$ and 40 wt-% KNO_3, so called "Solar Salt" (see Tab. 3), contained in a 3-tank storage system. For this purpose, cold molten salt with a temperature of 306 °C is pumped through additional shell-and-tube heat exchangers and is heated to the design temperature of the hot storage tank of 528 °C. Because of the nonlinear trend (see Fig. 1 (b) and (c)) of the heat capacity flow of superheated steam, a smaller molten salt mass flow is necessary in the colder than in the hotter sensible storage section. The integral difference of the mass flow is stored inside a third intermediate tank at a temperature of 400 °C. With this approach, which was first proposed in [7], an optimized SHTES was developed within this work. The fundamental difference of the new system is that there is no preheating done inside the SHTES. This is possible because the exhaust steam from the reheater is used for preheating purposes inside an additional feedwater preheater of the PB. With this additional heat exchanger, it is possible that the remaining preheating occurs inside the LHTES.

TABLE 2. Thermal properties of PCM $NaNO_3$ [15]

Property	Value	
Density, liquid, 306 °C	1,908	kg/m³
Specific heat capacity	1.66	kJ/(kg·K)
Thermal conductivity	0.55	W/(m·K)
Heat of fusion	178	kJ/kg
Melting temperature	306	°C

TABLE 3. Thermal properties of the Molten Salt at 306 °C [16]

Property	Value	
Density	1,894	kg/m³
Specific heat capacity	1.5	kJ/(kg·K)
Thermal conductivity	0.5	W/(m·K)
Temperature cold tank	306	°C
Temperature interm. tank	400	°C
Temperature hot tank	528	°C

DESIGN PROCESS FOR LATENT HEAT ENERGY STORAGE SYSTEM

The LHTES consists of multiple vertical steel tubes equipped with aluminum fins. This enhancement of heat transfer is necessary in order to overcome low thermal conductivities of the alkali salts used as the PCM, as mentioned above. Especially during solidification of the PCM, the heat transfer is limited by the thermal conductivity of solid PCM and the absence of natural convection. A cost effective enhancement method is to employ extruded longitudinal fins. These fins can be mounted on the steel tubes with special steel clips as proposed by [11]. As proposed there, each finned tube is embedded in a hexagonal basic geometry. With a hexagonal design (see Fig. 2), multiple tubes can be packed inside a storage tank without additional PCM that is not reached by the fin structure. Based on the choice of the hexagonal basic geometry, two main targets have been investigated: a) the determination of optimum type of fin profile, i.e. the fin profile class for this application and b) the determination of the optimum distance between finned tubes, i.e. the tube pitch.

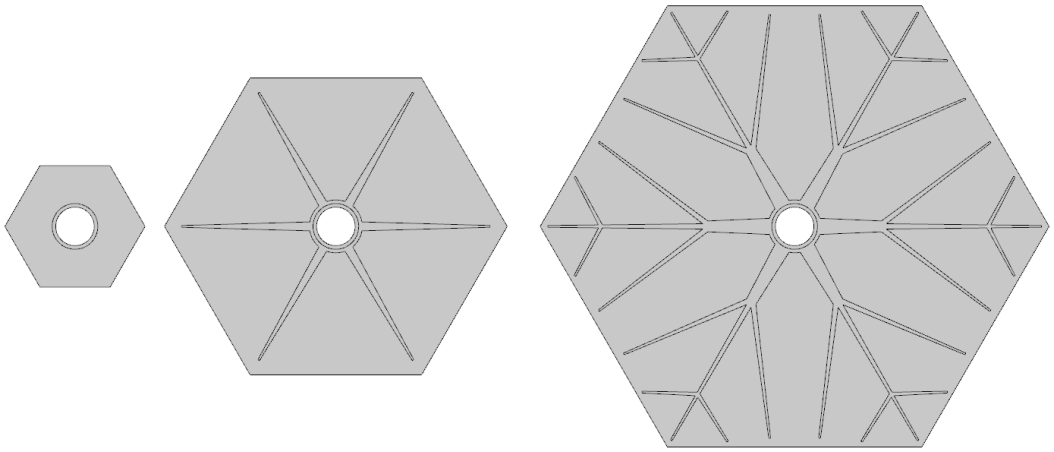

FIGURE 2. 2-D fin profiles embedded in hexagonal basic geometry; Geo-6A0, Geo-6A1 and Geo-6A4 with 67.5, 165 and 245 mm tube pitch, respectively.

The comparison is based on the specific product costs $C_{product}$ in €/kWh$_{th}$. These costs relate the product costs of one finned tube to the specific energy that is discharged from a completely molten PCM at solidification temperature within 7 hours. The discharged energy is obtained from a numerical simulation of a 2-D fin profile as shown in Fig. 2. These simulations are conducted with Comsol Multiphysics® applying a 10 K driving temperature difference between PCM's solidification temperature and the evaporation temperature of water of. The product costs include material costs for steel, aluminum and the PCM itself. Further, they include manufacturing costs for extruding the fin profiles, for connecting the fin profiles with steel tubes and for welding the steel tubes to a water/steam distribution system at both ends of the tube.

Many types of fin profile classes, including tubes without any fins, tubes with simple star fins and tubes with complex fin profiles were developed. In order to compare different profile classes, each class' optimum has to be determined. The results clearly show that specific product costs are at a minimum when the PCM solidifies simultaneously in all of the compartments between adjacent fins. Further, due to very high PCM costs, it is beneficial to discharge all the available energy within the discharge time of 7 hours. This behavior determines the size of the basic geometry that corresponds to the tube pitch. The optimum tube pitch for the three fin profile classes shown in Fig. 2 are at 67.5 mm, 165 mm and 245 mm for a tube without fins (Geo-&A0), a tube with a star-fin profile (Geo-6A1) and a complex fin profile (Geo-6A4), respectively.

Figure 3 compares these optimum profiles of each class based on the relative specific product costs. Tubes without fins provide specific product costs that are 52 % higher than the product costs of Geo-6A4. The optimum star-fin profile's costs are 22 % above those of Geo-6A4. These cost differences are mainly caused by the different tube pitches and thus the number of required tubes in order to provide a certain storage capacity. Compared to Geo-6A4, the total number of tubes increases by a factor of 2 and 14 for Geo-6A1 and Geo-6A0, respectively. Likewise, the welding costs increase by the same factor. The welding cost share of Geo-6A0 is 45.3 %, whereas this share is only 6.4 % and 4.9 % for Geo-6A2 and Geo-6A4, respectively. All in all, these results clearly demonstrate the techno-economic benefits of Geo-6A4 that is chosen as the basic design for the LHTES for this application.

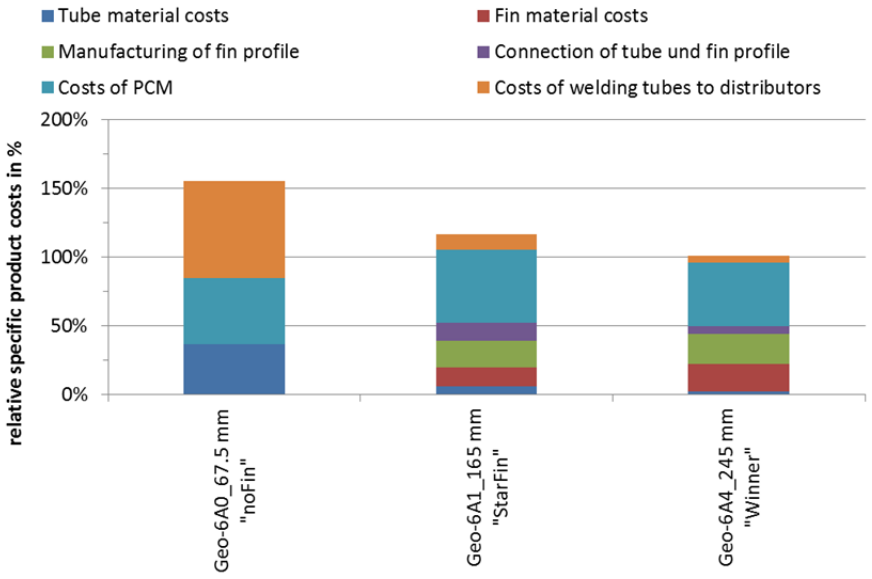

FIGURE 3. Fin profile comparison of different fin profile classes.

The profile Geo-6A4 was used for the transient calculation of the LHTES. For this purpose, the simulation methodology described in [14] was used to generate the charging power characteristic lines shown in Fig. 4 (a). The charging of the TES system is done in a fixed pressure mode, as in [10]. This means that the driving temperature difference is adjusted by the pressure of the water/steam inside the LHTES pipes. A higher pressure always results in a higher driving temperature difference.

For a comfortable handling of the characteristic line, the state of charge (SOC) is introduced in Eq. 1 and is calculated by division of the current and the maximum amount of energy at rated conditions. This means that if the LHTES is fully charged, the $SOC = 1$. An empty storage is denoted by a $SOC = 0$.

$$SOC = \frac{Q_{\text{LHTES}}}{Q_{\text{LHTES,DESIGN}}} \quad (1)$$

With the simulation results in Fig. 4 (a), it can concluded that a temperature difference of 15 K is the optimum for the charging process, because the charging power is higher than 75 MW for more than 50 % of the state of charge level. It would be possible to use a temperature difference of about 20 K for charging, but the characteristic is nearly the same. Therefore, it is not reasonable to increase the live steam pressure further.

During the discharging of the TES system, forced recirculation mode for the LHTES is applied as investigated in [10]. For this reason, a steam drum is used (not depicted in Fig. 1) to operate the TES system in a sliding pressure mode. Therefore, the evaporation pressure is dependent on the SOC and the retrieved power inside the LHTES (see Fig. 4 (b)).

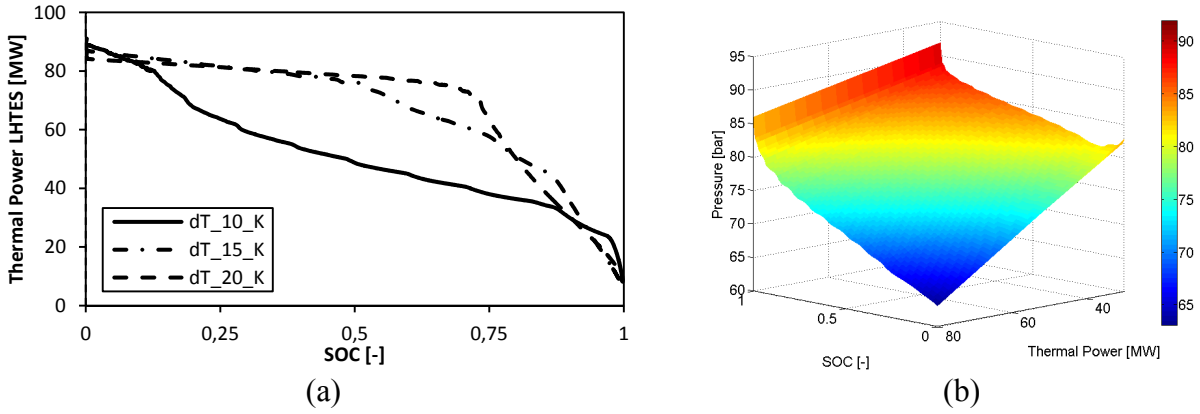

FIGURE 4. (a) Charging characteristic power curve of the LHTES for three different temperature differences for fixed pressure mode. (b) Discharging pressure characteristic map of LHTES for sliding pressure mode.

SYSTEM ANALYSIS RESULTS

With the discussed characteristic line, it is possible to develop a quasi-stationary system simulation model (see Fig. 5) of the DSG-power plant. The SF is not modeled for this kind of investigation, because only ideal charging and discharging cycles of the TES without the consideration of solar irradiance are investigated within this work. For the simulation of the SHTES, basic heat and mass transfer equations are set and solved within the calculation of the DSG power plant model.

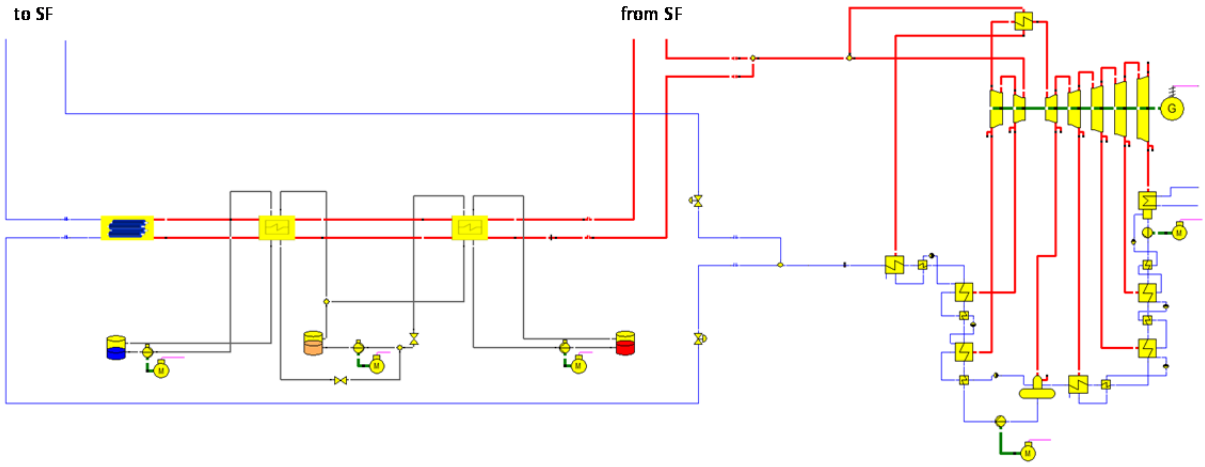

FIGURE 5. Ebsilon simulation model for the DSG power plant with PB and sensible/latent TES.

In Fig. 6, the calculated trends of the charging (a) and discharging (b) process of the total TES, the LHTES and the SHTES are shown. During the charging process, the LHTES operates in a fixed pressure mode with a constant temperature difference between condensation temperature and the PCM. Based on the transient behavior of a LHTES, the thermal charging power decreases over time. This effect is caused by the low thermal conductivity of the used PCM $NaNO_3$ and results in a reduced water/steam mass flow through the TES system. Because of the mass flow reduction, the stationary SHTES thermal power, i.e. the molten salt mass flow, is also reduced to meet the scheduled tank temperatures of the intermediate and hot storage tank. The discharging process is performed with a sliding pressure mode, in order to better operate the turbine. Therefore, it is possible to adjust the evaporation pressure inside the LHTES pipes for the required thermal power of the system. This steam pressure is correlated to the steam mass flow by the swallowing capacity of the steam turbine. The described context between PB and TES system results in a slight decrease of the thermal power of the TES system, as depicted.

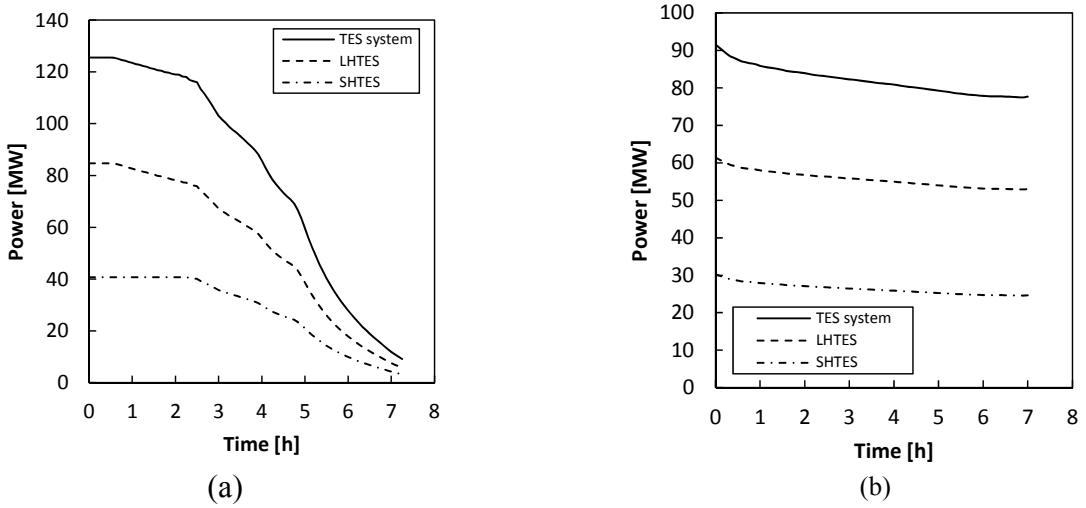

FIGURE 6. (a) Ideal charging and (b) discharging cycle of the presented storage system for DSG power plants.

In Tab. 4 a summary of the performed system analysis with the presented simulation model is given. It is obvious that the SHTES cannot be discharged in the same time as the LHTES. This is caused by the partial load behavior of the heat exchanger of the SHTES during discharging. Since the amount of sensible energy is very small and can be used for preheating purposes during startup, this effect is acceptable.

TABLE 4. Summary of the main parameter results of the system analysis.

		Charging	Discharging
Time	h	7.25	7
Thermal energy LHTES	MWh	390	390
Thermal energy SHTES	MWh	200	185
PB power (electrical)	MW	50	35.7-28.3
PB cycle efficiency	%	41.8	38.4-36.4

CONCLUSION

Due to the complex geometry of the LHTES, an optimization process is necessary for the determination of an optimal design for the fin geometry and the internal tube pitch. With this fundamental design work, it is possible to determine the behavior of the LHTES and design the SHTES.

With the presented results within this paper, the interdependency of the TES system and the other subsystems of the DSG power plant process, including the solar field and power block, is shown. This strong influence on the TES system depends mainly on the pressure dependency of the water/steam cycle. It is therefore very important to design the complete power plant process around the PCM melting temperature. The generated results also show the combined discharge of the TES and the steam turbine in a sliding pressure operation mode, which was identified as

the best mode for discharging such a storage system with a LHTES for the heat of evaporation respectively condensation.

It was demonstrated that it is possible to satisfactorily combine a stationary 3-tank SHTES and a transient LHTES. In a next step, the complex model used here has to be simplified for the calculation of longer time series. This is necessary for the calculation of the annual yield of a CSP plant with DSG and the determination of the additional benefit of a DSG power plant with TES system compared to a reference DSG power plant without such a TES.

ACKNOWLEDGMENTS

The authors would like to thank the German Federal Ministry for Economic Affairs and Energy for the financial support given to the DSG-Store project (Contract No. 0325333A and 0325333D).

REFERENCES

1. A. Khenissi, D. Krüger, T. Hirsch, K. Hennecke, *Return of Experience on Transient Behavior at the DSG Solar Thermal Power Plant in Kanchanaburi, Thailand*, Energy Procedia, No. 69 (2015) pp. 1603-1612.
2. F. Dinter, D. Mayorga Gonzalez, *Operability, reliability and economic benefits of CSP with thermal energy storage: first year of operation of ANDASOL 3*, Energy Procedia, No. 49 (2014) pp. 2472-2481.
3. M. Eck, N. Benz, F. Feldhoff, Y Gilon, Z. Hacker, T. Müller, K.-J. Riffelmann, K. Silmy, D. Tislaric, *The Potential of Direct Steam Generation in Parabolic Troughs – Results of the German Project DIVA*, Proceedings of the 14th Biennial CSP Solar Paces Symposium 2008, Las Vegas, USA.
4. J. F. Feldhoff, K. Schmitz, Eck M., L. Schnatbaum-Lauman, D. Laing, F. Ortiz-Vives, J. Schulte-Fischedick, *Comparative System Analysis of Direct Steam Generation and Synthetic Oil Parabolic Trough Power Plants with Integrated Thermal Storage*, Solar Energy, No. 86 (2012) pp. 520-530.
5. B. Koretz, L. Afremov, O. Chernin, C. Rosin, *Molten Salt Thermal Energy Storage for Direct Steam Tower Systems*, Solar Paces 20.-23. Sept 2011. Granada, Spain.
6. D. Laing, C. Bahl, T. Bauer, D. Lehmann, W.-D. Steinmann, *Thermal energy storage for direct steam generation*, Solar Energy, No. 85 (2011) pp. 627-633.
7. M. Seitz, P. Cetin, M. Eck, *Thermal storage concept for solar thermal power plants with direct steam generation*, Energy Procedia, No. 49 (2014) pp. 993-1002.
8. R. Tamme, T. Bauer, J. Buschle, D. Laing, H. Müller-Steinhagen, W.-D. Steinman, *Latent heat storage above 120°C for applications in the industrial process heat sector and solar power generation*, International Journal of Energy Research 2008 Vol. 32, pp. 264–271.
9. V. Aga, A. Ehrsam, E. Boschek, M. Simiano, *Adaptation of a direct steam solar tower plant with molten salt storage for optimum value creation under different incentive schemes*, Energy Procedia, No. 49 (2014) pp. 1097-1106.
10. D. Laing, M. Eck, M. Hempel, M. Johnson, W.-D. Steinmann, M. Meyer-Grünefeldt, M. Eickhoff, *High Temperature PCM Storage for DSG Solar Thermal Power Plants Tested in Various Operating Modes of Water/Steam Flow*, Solar Paces 11.-14. Sept. 2012, Marrakech, Morocco.
11. D. Laing, T. Bauer, N. Breidenbach, B. Hachmann, M. Johnson, *Development of high temperature phase-change-material storages*, International Journal of Applied Energy 2013 Vol. 109 pp. 497 – 504.
12. R. Yogev, A. Kribus, *Operation strategies and performance of solar thermal power plants operating from PCM storage*, Solar Energy, No. 95 (2013) pp. 170-180.
13. T. Hirsch, A. Khenissi, *A systematic comparison on power block efficiencies for CSP plants with direct steam generation*, Energy Procedia, No. 49 (2014) pp. 1165-1176.
14. M. Johnson, J. Vogel, M. Hempel, B. Hachmann, A. Dengel, *Design of High Temperature Thermal Energy Storage for High Power Levels*, Greenstock 2015, Beijing, China.
15. T. Bauer, D. Laing, R. Tamme, *Characterization of Sodium Nitrate as Phase Change Material*, International Journal of Thermophysics, Vol. 33 (2013) pp. 91-104.
16. J.E. Pacheco, *Final Test and Evaluation Results from the Solar Two Project*, 2002, Sandia Report SAND2002-0120.